DARK CURRENTS FOR CEBAF LINACS*

Byung C. Yunn

Continuous Electron Beam Accelerator Facility

12000 Jefferson Avenue, Newport News, VA 23606, USA

Abstract

Continuing on our numerical study[1] of field emitted electrons from a superconducting CEBAF cavity we have identified all possible emission sites, magnitudes, and the energy profile of dark currents expected at CEBAF under nominal operating conditions. We find that most electrons do not survive beyond a single cryomodule which includes eight 5-cell superconducting cavities. However, some electrons can be accelerated through many cryomodules, ending up with an energy close to 100 MeV. However, no field emitted electrons can be recirculated along with an electron beam generated at the gun, due to the limited energy acceptance of CEBAF recirculation arcs.

I. INTRODUCTION

In our previous study[1], we found that most field emitted electrons from a CEBAF superconducting cavity were likely to stay in the cavity where they originated. However, some field emitted electrons could be accelerated to adjacent cavities when emitted from a few selected locations at a proper phase. Futhermore, we have identified all such emission sites in the CEBAF cavity which could become a potential source of dark currents. Our study, however, was not complete in that the tracking of electrons was not possible beyond a single cavity at the time. Dark current was estimated by calculating characteristics of a field emitted electron bunch leaving the cavity through open beam pipe. The arrival times of such a bunch at neighboring cavities determine whether the bunch can keep pace with the nominal electron beam. Even though we expect that forward moving field emitted currents from the linacs under the most favorable phase relationship with subsequent cavities in downstream cryomodules will be intercepted at the spreaders (and backward currents at the recombiners, respectively) due to low energy acceptance of less than one percent level of such beam transport modules, it is important to find out what actually happens to all dark current candidates when more than a single cavity is involved. In this paper we report on our study of following electrons throughout CEBAF linacs assuming the beam injection at 45 MeV. There is a chicane at the entrance to the linac which prevents dark currents originated at the injector reaching the linac.

II. A CEBAF CRYOMODULE

Cavities in a CEBAF cryomodule are arranged in a particular way in order to minimize emittance degradation due to rf coupler kicks. It is helpful to differentiate CEBAF cavities into 4 different groups for the purpose of describing such an arrangement, even though a CEBAF cavity has only a single configuration with no

variation in its assembly with FP and HOM couplers. A sketch of a 5-cell cavity which belongs to a group of type I cavities is shown in the following Fig. 1. A type II (III and IV respectively)
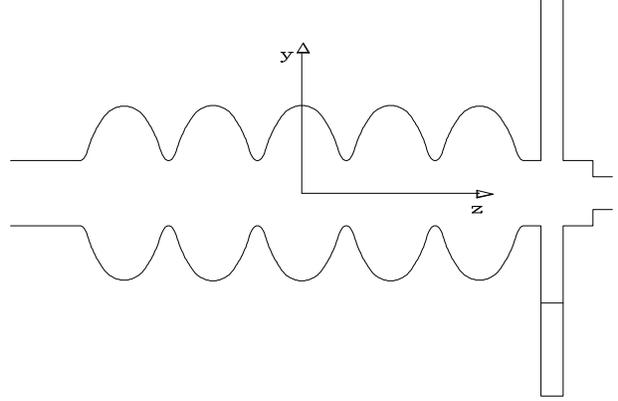
Figure. 1. Type I cavity: positive x-axis is into the paper.

cavity is defined as a type 1 cavity rotated by $180°$ about the +y axis (+z and +x axis respectively). In a cryomodule, we have 8 cavities in the following order:

$$\text{I - II - III - IV - III - IV - I - II} \qquad (A)$$

Our trajectory program(FEET) requires electromagnetic fields in whole CEBAF linacs as an input. This problem is manageable because cavities are all independently powered and cross talks between cavities[2] are negligible at the operating 1497 MHz mode. First, we calculate fields for a type I cavity numerically with the computer codes URMEL and MAFIA[3]. (For a practical reason, we had to divide the cavity into two regions: one with an axial symmetry and the other with no such symmetry.) Second, fields for other types of cavities are obtained from fields for the type I cavity by the symmetry consideration. Type II:

$$
\begin{aligned}
E_x^{II}(x, y, z) &= -E_x^I(-x, y, -z) \\
E_y^{II}(x, y, z) &= E_y^I(-x, y, -z) \\
E_z^{II}(x, y, z) &= -E_z^I(-x, y, -z)
\end{aligned}
\qquad (1)
$$

Type III:

$$
\begin{aligned}
E_x^{III}(x, y, z) &= -E_x^I(-x, -y, z) \\
E_y^{III}(x, y, z) &= -E_y^I(-x, -y, z) \\
E_z^{III}(x, y, z) &= E_z^I(-x, -y, z)
\end{aligned}
\qquad (2)
$$

Type IV:

$$
\begin{aligned}
E_x^{IV}(x, y, z) &= E_x^I(x, -y, -z) \\
E_y^{IV}(x, y, z) &= -E_y^I(x, -y, -z) \\
E_z^{IV}(x, y, z) &= -E_z^I(x, -y, -z)
\end{aligned}
\qquad (3)
$$

and similar transformations for magnetic fields.

III. TRACKING THROUGH LINACS

How the program FEET handles a field emitted electron in a CEBAF cavity can be found in ref. [1]. When an electron enters a neighboring cavity through the beam pipe, forces acting on the particle are calculated from the electromagnetic fields in the cavity performing field transformations described in Eqs. (1) to (3) depending on the type of the cavity. In addition rf phase must be also adjusted. Assuming that all cavities in the linacs are set up for a maximal energy gain of 2.5 MeV per cavity, absolute phases (in units of degrees at 1497 MHz) of 8 cavities in a cryomodule at time equal to zero are 0, -90, 165.936, 75.936, -28.127, -118.127, 137.809, and 47.809, respectively, in the order noted in the layout (A) of those 8 cavities in section II. The leftmost cavity of (A), which is of the type I, is chosen as the reference here. Also, there is an rf phase shift of 76.708 degree between the last cavity in a cryomodule and the first cavity in the next cryomodule . Furthermore, in the warm region between two cryomodules there is a quadrupole for focusing the electron beam, which was turned on in the simulation. The linac lattice is a FODO type with 120 degree phase advance per cell for the 1st pass beam. Focussing effects of a quadrupole are easily simulated with the 1st order transfer matrix. We also mention aperture limits in linacs which are 3.0 inches in cavities and 1.5 inches in beam pipes, loosely stated. (The program FEET treats this in complete detail.)

IV. RESULTS

For the present study, we scan the surface of the first two cavities (They are of the type I and II, respectively. For convenience of notation, we will simply refer to them as cavity I and cavity II) of the first cryomodule in the North linac for field emission at an accelerating gradient of 5 MV/m only. It is expected that dark currents containing the highest energy electron bunches have most likely originated from these two cavities because they have the largest number of downstream cavities available. 5 MV/m is the design value for the CEBAF cavity gradient. In order to obtain a detectable field emitted electron current at this field intensity we assume cavities with field enhancement factor β=300. According to Fowler-Nordheim[4] theory, the current density J in A/m^2 is given by

$$J = \frac{1.54 \times 10^6 (\beta E_{\text{surf}})^2}{\phi} \exp(-\frac{6.83 \times 10^3 \phi^{1.5}}{\beta E_{\text{surf}}}) \quad (4)$$

where E_{surf} is the surface electric field in MV/m and ϕ is the work function of the metal surface in eV. For niobium we take $\phi = 4$ eV. As in our previous study, the emission from a given site is normalized to a total dissipated power of 1 Watt. In other words, $A_E \int J(\theta) E_{\text{kin}}(\theta) d\theta = 2\pi$ W, where $J(\theta)$ is the current density determined with the instantaneous field at rf phase θ, $E_{\text{kin}}(\theta)$ is the impacting energy of the electron emitted at that phase, and the integration runs from 0 to π or π to 2π depending on the location of the site in the cavity. Average impact energy is determined by $\int J(\theta) E_{\text{kin}}(\theta) d\theta / \int J(\theta) d\theta$.

We can see a typical example of generation of dark current from Fig. 2. Trajectories of electrons emitted from a site in cavity I (see the site c in Fig. 3) at all phases are shown. Most electrons

with wrong phases fan out ending at nearby cells, while a small batch of electrons emitted at right phases escape to the downstream cavity II and beyond. We should mention that a piece of beam pipe about a half meter long, which is not pictured here, connects the top and the bottom portions of Fig. 2 to complete the cryomodule. The electron bunch essentially goes through the center of the beam pipe segment in cavities downstream of it. Dark current in the particular case shown in Fig. 2 terminates at the 19th cavity with an energy gain of about 36 MeV.
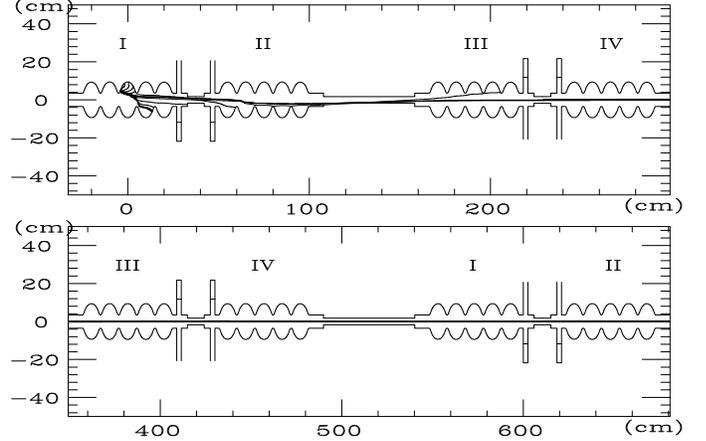
Figure. 2. An example of dark current generation in a CEBAF cryomodule at 5 MV/m gradient. Roman letters on top of cavities specify the types of the cavities as explained in section II.

We have identified all emission sites on the surface of cavity I and II which could serve as a source of dark current. In this paper we report only on those sites which produce field emitted electrons traveling downstream toward the end of the linacs. A complete list of all such sites with a brief note on some characteristics of electron bunches which form dark currents can be found in the following two subsections. In Figs. 3 and 4 we also present pictorially locations of the emission sites in the cavity I and II, respectively. An emission site is really a cylindrically symmetric thin strip of the cavity surface typically about a few mm wide. A vertical line in the figures specifies the center position of such a strip. In the following each emission site is represented by a letter (from a to m) assigned next to a vertical line.

A. Emission Sites at Cavity I
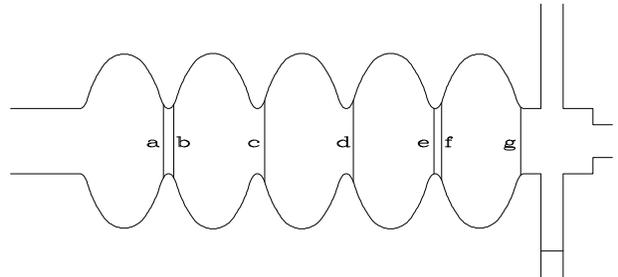
Figure. 3. Dark current emission sites located in the cavity I. Vertical lines represent thin strip regions as explained in the text.

Site a: We find two distinct phase windows, one about 0.5 deg wide delivering I_{avg} = 30 nA and power of 10 mW, and another 1.0 deg wide with I_{avg} = 160 nA and power of 40 mW. Most electrons terminate at the cavity II.

Site b: The region consists of two narrow strips about 2 mm apart. In the left strip we find two phase regions, one about 0.75 deg wide with I_{avg} = 0.5 nA and power of 0.2 mW (all power to the cavity II), and another about 0.5 deg wide with I_{avg} = 0.3 nA and power of 0.2 mW. In the latter case electrons travel up to the 7th cavity but attain maximum energy of only 2.6 MeV. In the right strip, a phase window of 15 deg produces I_{avg} = 0.3 nA and power of 0.12 mW with all electrons ending up on the cavity II.

Site c: We find two distinct phase regions, one about 2.5 deg wide with I_{avg} = 16 nA and power of 6 mW, and another 18.0 deg wide with I_{avg} = 5 nA and power of 3 mW. Electrons mostly terminate either at the 2nd or at the 3rd cavity except a small fraction of them (about 10 pA) reaching to the 19th cavity with a peak energy of 36 MeV.

Site d: There exist three distinct phase regions, one about 7.5 deg wide with I_{avg} = 9 pA and power of 0.02 mW, and another about 4.0 deg wide with I_{avg} = 0.4 nA and power of 1 mW with electrons reaching up to the 3rd cavity. The last one is about 2.5 deg wide with I_{avg} = 36 pA with a negligible power of 0.01 mW even though electrons travel to the 7th cavity.

Site e: We find a phase region of about 1 deg wide with I_{avg} = 19 nA and power of 12 mW. About 1 nA of electrons traverse a whole cryomodule only to be lost in the warm section while most electrons do not survive beyond the 3rd cavity. Peak energy achieved is 15 MeV.

Site f: A phase window of about 5 deg wide generates I_{avg} = 72 nA and power of 62 mW. About 2 nA of electrons travel to the 2nd cryomodule attaining a peak energy of 32 MeV.

Site g: The region consists of two strips 2 mm apart. In the left strip we find two 3 deg wide phase regions, one with I_{avg} = 0.5 μA and power of 36 mW, another with I_{avg} = 2 μA and power of 380 mW. Dark current terminates at the 3rd cavity. In the right strip, we also have two windows, one about 10 deg wide with I_{avg} = 8 μA and power of 615 mW delivered to nearby two cavities, another about only 0.1 deg wide with I_{avg} = 72 nA and power of 1.5 W with current extending to the 21st cavity.

B. Emission Sites at Cavity II
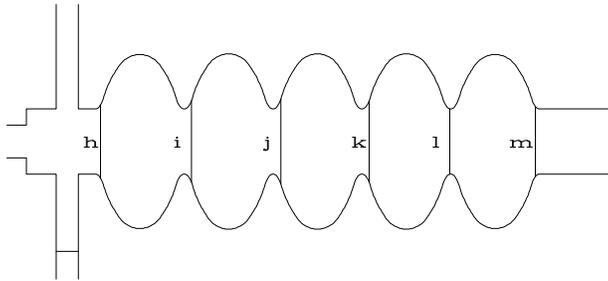
Figure. 4. Dark current emission sites at the cavity II.

Site h: There exists a phase window of about 0.1 deg width. Most electrons do not survive beyond the 3rd cavity, but a few of them reach to the 28th cavity attaining energy of 48 MeV. However, the current is extremely small and the power is negligible.

Site i: We find two phase regions, one about 20 deg wide with only I_{avg} = 0.1 pA (most power to the 3rd cavity), another about 5 deg wide with a negligible power of 10nW despite some electrons traversing a whole cryomodule and attaining a peak energy of 13 MeV.

Site j: A phase window about 0.5 deg wide exists. Electrons are accelerated to the 34th cavity attaining a peak energy of 75 MeV. However, power is only about 7 nW.

Site k: We find two phase regions, one about 10 deg wide with I_{avg} = 0.3 nA and power of 0.5 mW (about 0.5 pA of electrons reach the 4th cryomodule gaining a peak energy of 30 MeV), and another about 0.1 deg wide with electrons accelerated to the 23rd cavity. 45 MeV energy gain is achieved, but power is negligible.

Site l: I_{avg} = 16 nA and power of 2.5 mW is produced from a phase window about 1 deg wide. Almost all electrons are lost in the 3rd cavity.

Site m: There exit two distinct phase windows only about 0.1 deg wide, one with I_{avg} = 80 nA and power of 50 mW, another with I_{avg} = 50 nA and 30 mW. Most power is delivered to cavities in the latter part of the first cryomodule.

V. CONCLUSION

From the result presented here, we can safely assert that none of field emitted electrons can be recirculated along with an electron beam generated at the gun, due to the limited energy acceptance of CEBAF recirculation arcs.

References

[1] B. C. Yunn and R. M. Sundelin, *Proc. 1993 Particle Accelerator Conf.*, 1092 (1993).
[2] B. C. Yunn, "A Cross Coupling between Cavities," CEBAF TN-80 (1988).
[3] R. Klatt *et al.*, *Proc. 1986 Linear Accelerator Conf.*, 276 (1986).
[4] R. H. Fowler and L. Nordheim, *Proc. R. Soc. London* **A119**, 173 (1928).